Iran J Sci Technol Trans Sci (2020) 44:903–910
https://doi.org/10.1007/s40995-020-00876-6

RESEARCH PAPER

# The Influence of Time-Dependent Aging Process on the Thermodynamic Parameters and Microstructures of Quaternary $Cu_{79}$–$Al_{12}$–$Ni_4$–$Nb_5$ (wt%) Shape Memory Alloy

Ibrahim Nazem Qader[1,2] · Ercan Ercan[3] · Bahar Ali Mohammed Faraj[1] · Mediha Kok[1] · Fethi Dagdelen[1] · Yildirim Aydogdu[4]

Received: 28 January 2020 / Accepted: 17 April 2020 / Published online: 2 May 2020


**Abstract**
The heat treatment techniques are significant methods for improving metals and alloys. Particularly, it is important to control transformation temperature and improve mechanical and physical properties of materials. There are two important parameters that can be controlled, which are temperature and time of aging. In this study, a quaternary $Cu_{79}$–$Al_{12}$–$Ni_4$–$Nb_5$ (wt%) alloy was produced using arc melting under an atmosphere control. The alloy was aged isothermally at 1073 K for 1, 2, 3, 6, 12, and 24 h. The map of constituents showed that neither Cu contributed in Nb-rich phases nor Nb dissolved in the matrix. The martensitic phase transformation for as-casted and aged specimens was carried out using a DSC device. The phase transformation was generally shifted to the higher temperature by increasing the time of aging, but the alloy lost its shape memory feature when it was aged for 24 h. XRD and optical microscopy were utilized to investigate characterizations of the alloy. Additionally, the aging introduced multiphases in the alloys and the intensity of XRD peaks was increased by increasing the time of aging up to 3 h.

**Keywords** Cu–Al–Ni–Nb · Shape memory alloy · Aging process · Microstructure · Thermal analysis

## 1 Introduction

In recent decades, shape memory alloys (SMAs) have made a significant contribution to the high technological application, because they have shown a remarkable noise reduction, high strain recovery, and comparably high vibration damping (Graesser and Cozzarelli 1991; Mabe 2008; Qader et al. 2019a, b). These alloys are classified into some families, such as NiTi-based and Cu-based SMAs, where they get more attention from researchers and engineers. Since their crystal structure can be flipped between two solid phases (austenite and martensite), the energy of deformation can be stored in the martensite and it can be released through austenite phase transformation.

Although NiTi-based alloys are more prominent in the industrial fields, they have a comparably high price and mostly can be used for low-temperature applications. On the other hand, Cu-based SMAs are considered as an alternative for some other applications. Cu–Al–Ni-based SMAs have demonstrated phase transformation between − 200 and 200 °C (Čolić et al. 2010), while the production technique and alloying with new elements can enhance the range of phase transformation and other some other physical characteristics of the alloy (Dagdelen et al. 2019a, b; Qader et al. 2019a, b; Vajpai et al. 2013).

Saud et al. (2016) investigated the effect of different aging conditions on microstructural and mechanical properties of quaternary CuAlNiTi SMAs. They found that the increase in both temperature and aging time could shift phase transformation temperatures to higher temperatures.

✉ Ibrahim Nazem Qader
inqader@gmail.com

[1] Department of Physics, Faculty of Science, Firat University, Elazig, Turkey

[2] Department of Physics, College of Science, University of Raparin, Sulaymaneyah, Iraq

[3] Department of Physics, Science Faculty, Bitlis Eren University, Bitlis, Turkey

[4] Department of Physics, Science Faculty, Gazi University, Ankara, Turkey

The microstructural phase was affected through the aging process; thus, the tensile strength and other mechanical characteristics were influenced by keeping the alloys in different temperatures and various times. Suresh and Ramamurty (2008) found that the fraction of precipitate increased with increasing aging temperature, and thus, the damping of the alloy was decreased. There is not any investigation about the effect of aging on the microstructural and thermal characteristics of Cu–Al–Ni–Nb in the literature.

In this study, a quaternary Cu–Al–Ni–Nb shape memory alloy has been obtained using the arc-melting technique. The alloy has been investigated for a controlled isothermally aging process. The crystal structural analysis has been carried out using XRD measurement, and surface morphology has been scanned with a metallurgical microscope (optical microscope). In addition, the thermal analysis of the CuAlNiNb SMA has been studied using differential scanning calorimetry (DSC). Some other related calculations have been done to broaden the scope of the study.

## 2 Materials and Experimental Procedures

To produce the quaternary Cu–Al–Ni–Nb shape memory alloy, a particular amount of metallic powders with high purity were weighed with highly sensitive balance (SCALTEC Analytical balance SBC). The alloy consisted of copper, aluminum, nickel, and niobium with 79, 12, 4, and 5 weight percent (wt%), respectively. The powders were stirred well in a closed compartment to obtain a desired alloy with comparably high homogeneity. Pelletization of powders was carried out under 5 MPa compression, and the pellet was melted in an arc melter in an argon atmosphere. After the obtained ingot was cooled to room temperature in the natural atmosphere, it was cut into eight different samples to apply the aging process. In Table 1, all specimens with the experimental conditions are summarized. The alloy was aged at 1073 K for 1, 2, 3, 6, 12, and 24 h followed by quenching in the ice-brined medium.

**Table 1** The nominal codes and a summary of the applying procedure on the Cu–Al–Ni–Nb shape memory alloy

| Alloys' code | Temperature (K) | Time (h) | Quenching procedure |
|---|---|---|---|
| 0 h | – | – | – |
| 1 h | 1073 | 1 | Ice brined |
| 2 h | 1073 | 2 | Ice brined |
| 3 h | 1073 | 3 | Ice brined |
| 6 h | 1073 | 6 | Ice brined |
| 12 h | 1073 | 12 | Ice brined |
| 24 h | 1073 | 24 | Ice brined |

The phase transformation characteristics for as-casted and aged alloys were accomplished with differential scanning calorimetry (Perkin Elmer Sapphire). The DSC was run with 10 K/min and nitrogen gas flowed throughout the running process. Additionally, the effect of aging on the crystal structure of the Cu–Al–Ni–Nb alloy was studied through an X-ray diffraction device (Rigaku D/Max-B Geigerflex). In addition, the microstructure and the precipitation of the different constituents were investigated using optical microscopic (PRIOR Model N334 Incident Light Metallurgical Trinocular Microscope) and mapping (EVO 40XVP) technique.

## 3 Results and Discussion

The distribution of the alloy's constituents is shown in Fig. 1. The dominant Cu elements have distributed all over the alloys except in some particular positions, which seems to be filled by Nb elements. Ni elements homogenously have distributed, which means nickel could be presented as a solid solution, while Al, on the other hand, could be dissolved in the matrix and presented in the same microstructures that Nb elements have created.

The DSC measurements (Fig. 2) determined the phase transformation temperatures (TTs), which are listed in Table 2. It can be seen that the investigated alloys have TTs around 500 K which can be considered as a high-temperature shape memory alloy (HTSMA). The aging process shifted the TTs to the higher temperatures (Fig. 3), and after 24 h, the alloy evolves from a martensitic transformation to a non-martensitic transformation alloy, and the alloy lost its shape memory properties. These results show that the thermal aging method significantly affects the transformation temperatures of CuAl-based SMAs.

In another study, Balo and Sel (2012) also examined the effect of aging time (0–7 h) on the CuAlNi alloy and found that the TTs fluctuated. However, Benke and his friends (2007) found that the TTs of CuAlNi SMA were increased by increasing aging time. On the other hand, Zhou et al. (2017) reported that the coherence precipitates were the main reason for the emergence of the phase transformation in FeNiCoAlTaB.

The amount of latent heat (enthalpy change) needed for the phase transformation process is obtained from the area under the endothermic troughs and exothermic peaks of the DSC curves. The value of enthalpy change ($\Delta H$) was obtained through the DSC software program. Mathematically, the enthalpy change ($\Delta H$) of the phase transformation is represented by (Elrasasi et al. 2013; Kök et al. 2020; Recarte et al. 2004):

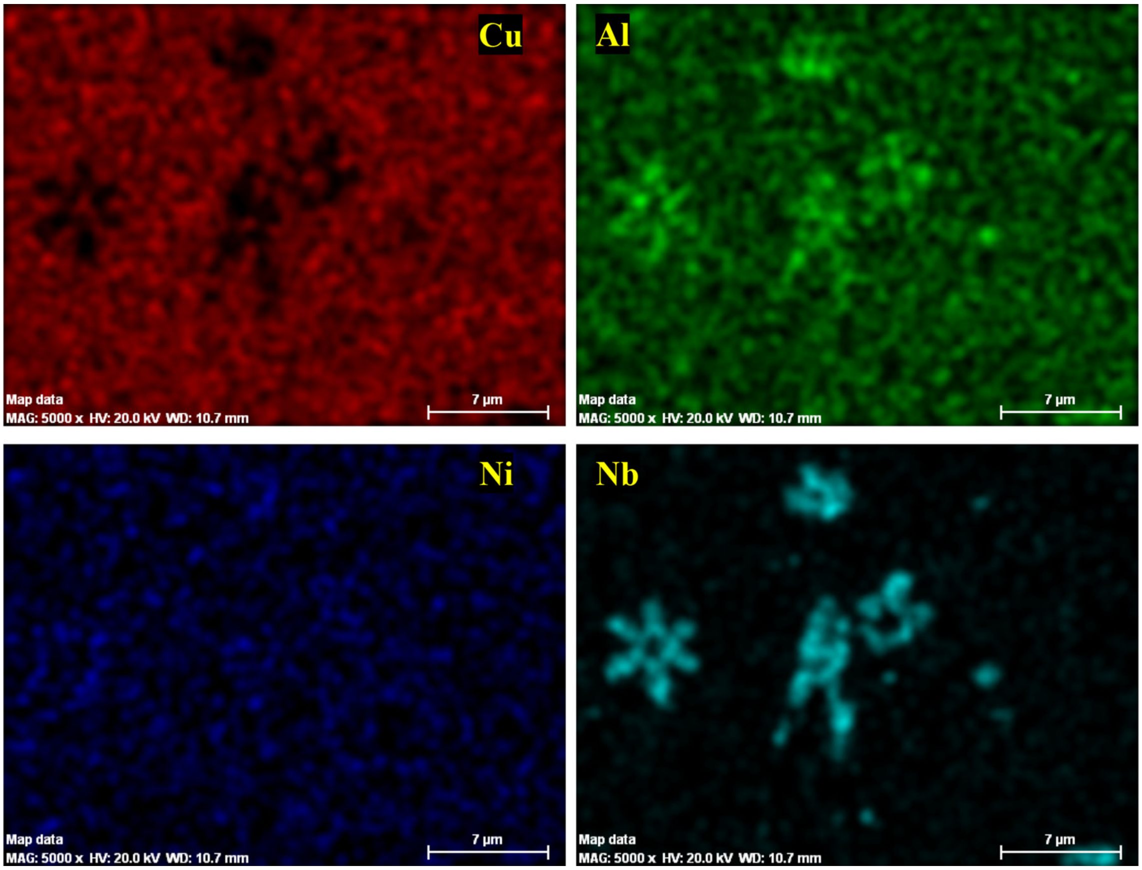


**Fig. 1** The obtained mapping for concentration of Cu, Al, Ni, and Nb constituents in the as-cast alloy

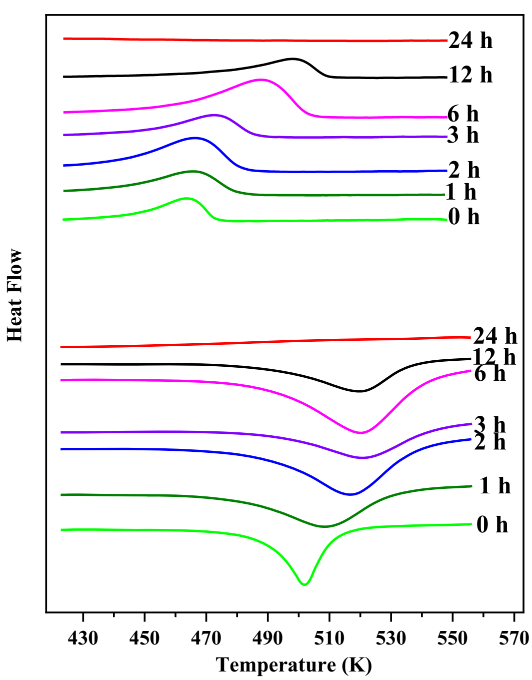


**Fig. 2** The DSC curves of the aged Cu–Al–Ni–Nb SMA

**Table 2** Phase transformation temperatures for all the aged Cu–Al–Ni–Nb shape memory alloys

| Name | $A_s$ (K) | $A_p$ (K) | $A_f$ (K) | $M_s$ (K) | $M_p$ (K) | $M_f$ (K) |
|---|---|---|---|---|---|---|
| 0 h | 481.2 | 501.8 | 512.4 | 473.2 | 464.4 | 436.5 |
| 1 h | 469.1 | 508.6 | 541.2 | 480.7 | 465.4 | 427.9 |
| 2 h | 477.3 | 517.3 | 546.9 | 481.2 | 466.8 | 435.6 |
| 3 h | 479.7 | 521.4 | 549.5 | 485.9 | 472.8 | 437 |
| 6 h | 479.4 | 520.3 | 556 | 503.6 | 489 | 456.1 |
| 12 h | 478.5 | 520.3 | 545.2 | 509.3 | 498.4 | 473.8 |
| 24 h | – | – | – | – | – | – |

$$\Delta S^{\mathrm{M}\to\mathrm{A}} = \int_{A_s}^{A_f} \frac{\mathrm{d}q}{\mathrm{d}T}\left(\frac{\mathrm{d}T}{\mathrm{d}t}\right)^{-1}\mathrm{d}T$$

or

$$\Delta S^{\mathrm{M}\to\mathrm{A}} = \int_{A_s}^{A_f} \frac{\mathrm{d}Q^{\mathrm{M}\to\mathrm{A}}}{T_o} = \frac{\Delta H^{\mathrm{M}\to\mathrm{A}}}{T_o} \quad (1)$$

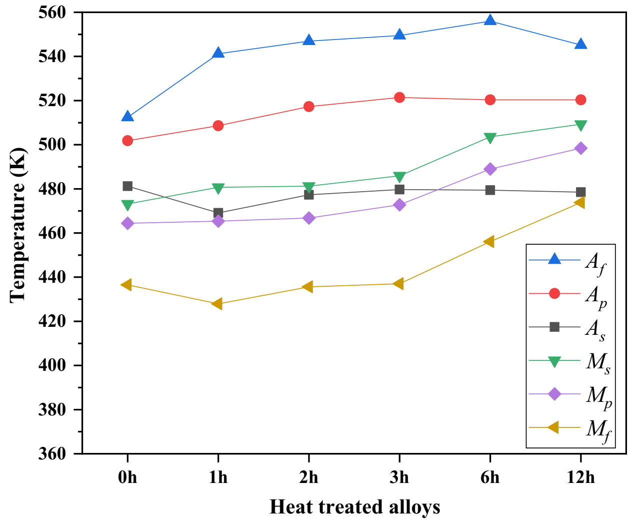


**Fig. 3** The obtained phase transformation temperatures for different aging times of the Cu–Al–Ni–Nb SMA

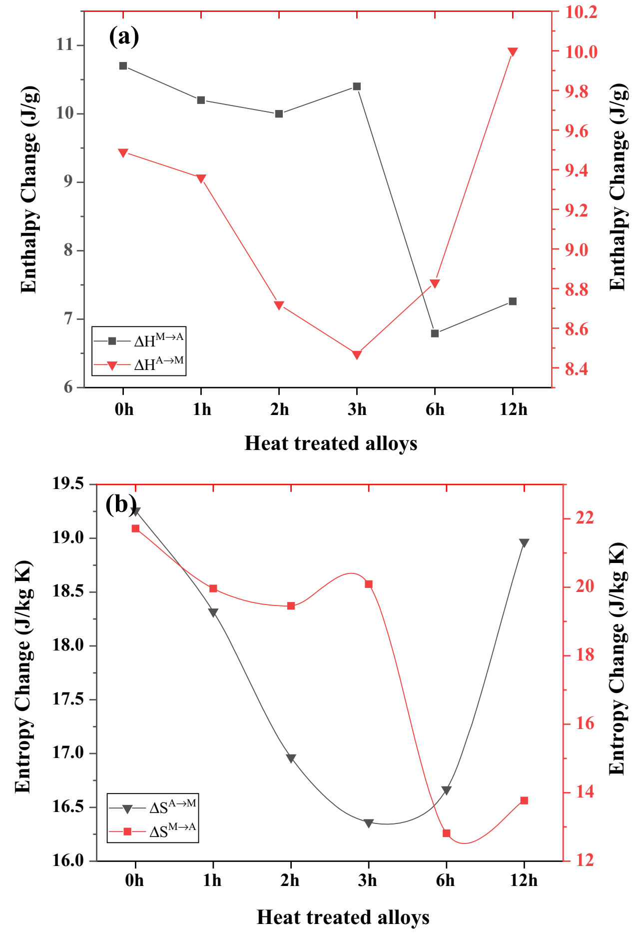


**Fig. 4** The enthalpy change and entropy changes of the aged Cu–Al–Ni–Nb SMA

where $\Delta S$ is the entropy change of martensitic phase transformation and $T_o$ is the temperature where Gibbs free energy for both austenite and martensite phase transformation is equal to zero $(T_o = (M_s + A_f)/2)$ (Dagdelen et al. 2019a, b; Kok et al. 2019). The enthalpy and entropy change values for all cases are listed in Table 3. Figure 4 presents the $\Delta H$ and $\Delta S$ for forward and reverse martensitic phase transformations, in which generally they decreased with increasing heat treatment. The $\Delta H^{A\to M}$ and $\Delta S^{A\to M}$ recorded the minimum value for 3-h aging at 1073 K. In different circumstances, Ii et al. (2009) investigated aging time and temperature for CuAl alloyed by different compositions of Mn. They have found that the time of aging increased TTs and enthalpy change of the alloys.

The energy associated with the martensitic phase transformation is known as Gibbs free energy of transformation ($\Delta G$). The pushing force at equilibrium temperature can be formulated as (Dagdelen et al. 2019a, b):

**Table 3** Enthalpy and entropy change obtained for aged Cu–Al–Ni–Nb alloys

| Name | $\Delta H_{M\to A}$ (J/g) | $\Delta H_{A\to M}$ (J/g) | $\Delta S^{M\to A}$ (J/kg K) | $\Delta S^{A\to M}$ (J/kg K) |
|---|---|---|---|---|
| 0 h | 10.7 | 9.49 | 21.71 | 19.26 |
| 1 h | 10.2 | 9.36 | 19.96 | 18.32 |
| 2 h | 10.0 | 8.72 | 19.45 | 16.96 |
| 3 h | 10.4 | 8.47 | 20.09 | 16.36 |
| 6 h | 6.79 | 8.83 | 12.82 | 16.67 |
| 12 h | 7.26 | 10.0 | 13.77 | 18.97 |
| 24 h | – | – | – | – |

$$\begin{aligned}\Delta G^{M\to A}(T_o) &= G^A(T_o) - G^M(T_o)\\ &= (H^A - T_oS^A) - (H^M - T_oS^M)\\ &= \Delta H^{M\to A} - (T_o\Delta S^{M\to A}) = 0\end{aligned} \quad (2)$$

where superscript A and M represent austenite and martensite, respectively. For the martensite phase transformation, Eq. (2) can be rewritten as (Dagdelen et al. 2020; Tatar et al. 2020):

$$\Delta G^{A\to M}(M_s) = \Delta G^{M\to A}(T_o) - \Delta G^{M\to A}(M_s) \quad (3)$$

or

$$\Delta G^{A\to M}(M_s) = -(T_o - M_s)\Delta S^{M\to A}. \quad (4)$$

Additionally, the elastic energy ($G_e$) can be calculated from subtracting Gibbs free energy for forward and reverse phase transformation (Acar et al. 2020; Kok et al. 2019):

$$G_e = \Delta G^{A\to M}(M_s) - \Delta G^{A\to M}(M_f) = (M_s - M_f)\Delta S^{M\to A}. \quad (5)$$

The calculated results for Gibbs free energy, elastic energy, equilibrium temperature, and temperature hysteresis ($M_f - M_s$) for as-casted and aged alloys are listed in Table 4. There were no calculations for the CuAlNiNb alloy aged for 24 h. Figure 5a shows that Gibbs free energy and temperature hysteresis of the alloy were closely related to each other. These parameters reached maximum values for 2–3-h aging at 1073 K and then by increasing the time of aging their values diminished. Elastic energy of the alloy attained the highest value for 1-h aging at 1073 K. The value of $G_e$ decreased and stayed nearly constant for 6 h of aging, and then, it decreased again for increasing aging time at that particular temperature.

Figure 6 shows the optical microscope (OM) images. There are flower-like precipitated phases spread all over the alloys. It was found that the flower-like phases are niobium-rich phases with no copper content and the Al and Ni were dissolved in the alloys. The matrixes consist of martensite thin discrete middle phase ($\beta_1'$). $\beta_1'$ has an 18R-type ordered structure (Araujo et al. 2017).

The crystal structural and various phases included in the as-casted and heat-treated Cu–Al–Ni–Nb SMAs are given in Fig. 7. The peaks were indexed with Refs. Ercan et al. (2020), Moghaddam et al. (2017), and Qader et al. (2019a, b). They showed that the matrix of the alloys is martensite ($\beta_1'$) phase with high-temperature cubic austenite phases, including $\alpha$ and $\beta_1$. $\beta_1'$, $\gamma'$, and $\beta_1$ phases that have order types of $DO_3$ ($BiF_3$), 18R ($Cu_3Al$), and 2H ($Cu_3Ti$) phases, respectively (Braga et al. 2017; Otsuka et al. 1979). Additionally, there is also $\gamma'$ phase, which appeared for all treated times and after 24 h it disappeared. The martensitic phase transformation can be defined as $\alpha$ and/or $\beta_1 \leftrightarrow \beta_1'$ and $\gamma'$. It can be seen that the as-casted alloy shows a single peak ($\beta_1'$), while the aged samples illustrate multipeaks with different phases. Besides, the intensity of the peaks was increased by increasing the time

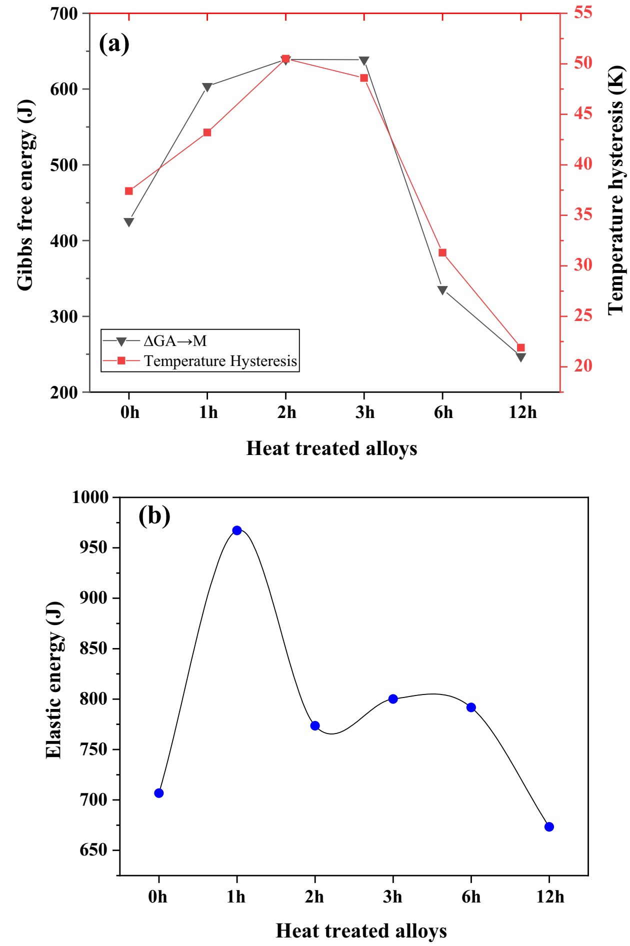


**Fig. 5** The calculated **a** Gibbs free energy and temperature hysteresis, and **b** elastic energy of the as-casted and aged Cu–Al–Ni–Nb SMA

of aging up to 3 h, and it again decreased for more aging times. Although the 24-h aged alloy did not show shape memory characteristic, it still has a crystalline phase.

The crystallite size of the alloys was calculated through the Scherrer equation (Buytoz et al. 2019; Shiva et al. 2015):

$$D = \frac{0.9\lambda}{B\cos\theta} \quad (6)$$

where $\lambda$ is the X-ray wavelength that has been used for the XRD measurement (for this study it was 1.5406 Å), $B$ is full width at half maximum (FWHM), and $\theta$ is the Braggs angle. The results of the calculations showed that the crystallite sizes dramatically decreased by applying heat treatment on the alloy (Fig. 8).

**Table 4** Temperature hysteresis ($H_t$), equilibrium temperatures ($T_o$), Gibbs free energy ($\Delta G$) for martensite phase transformation ($\Delta G^{A\rightarrow M}$), and elastic energy ($G_E$) for the Cu–Al–Ni–Nb shape memory alloy

| Name | Temperature hysteresis (K) | $T_o$ (K) | $\Delta G^{A\rightarrow M}$ (J) | $G_E$ (J) |
|---|---|---|---|---|
| 0 h | 37.4 | 492.8 | 425.6 | 706.7 |
| 1 h | 43.2 | 511.0 | 603.9 | 967.2 |
| 2 h | 50.5 | 514.1 | 639.0 | 773.5 |
| 3 h | 48.6 | 517.7 | 638.8 | 800.0 |
| 6 h | 31.3 | 529.8 | 335.8 | 791.7 |
| 12 h | 21.9 | 527.3 | 247.2 | 673.3 |
| 24 h | – | – | – | – |

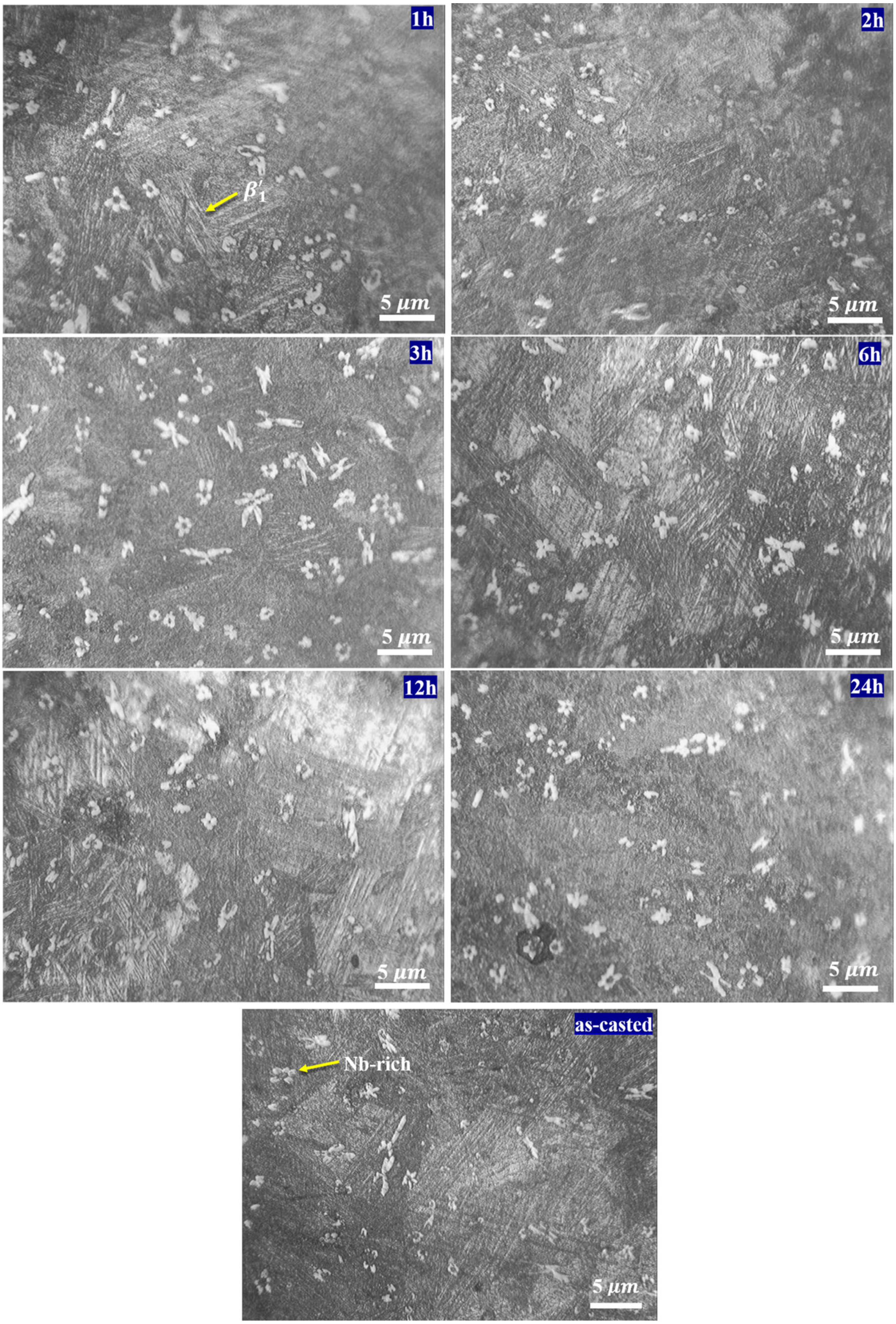


**Fig. 6** The optical microscopy images of the aged Cu–Al–Ni–Nb SMA

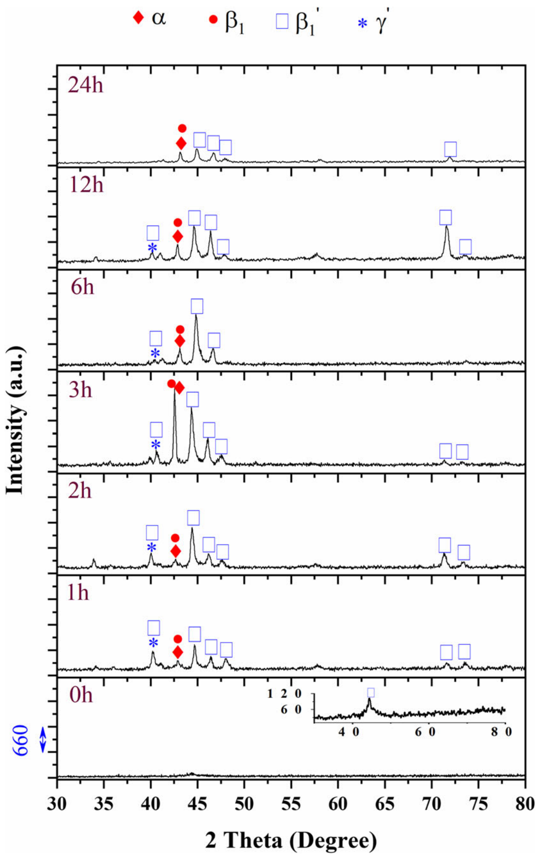


**Fig. 7** The XRD results of as-casted and the heat-treated Cu–Al–Ni–Nb SMAs

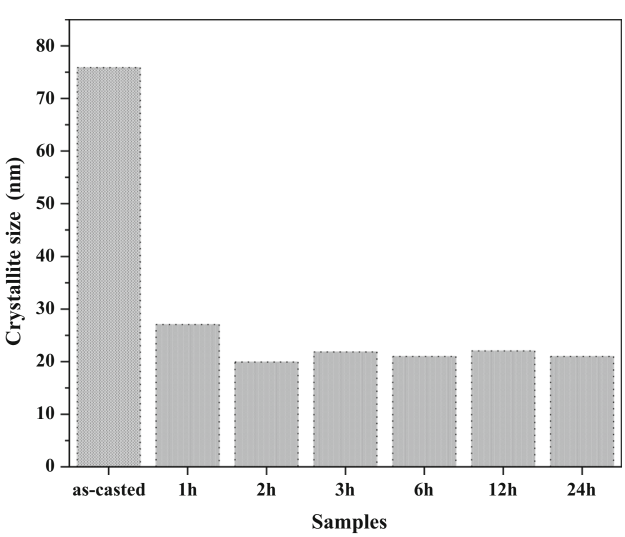


**Fig. 8** The crystallite size of the SMAs

## 4 Conclusions

A quaternary Cu–Al–Ni–Nb shape memory alloy was produced using the arc-melting technique. The alloy was aged for seven different aging times. The as-casted and other aged alloys were characterized using DSC, OM, and XRD. Additionally, some related calculations were performed. The important outcome of this study is as follows:

- The matrix phases showed martensite-$\beta_1'$ with some flower-like precipitations distributed all over the alloys.
- The map compositions of the alloy showed Nb elements were not dissolved in the matrix, but they precipitated some secondary phases.
- The phase transformation temperatures increased with increasing the time of aging.
- The enthalpy and entropy changes of the alloy recorded minimum value for 3-h aging, which could have the most stable phase transformation compared to the other cases.
- The alloy with 24-h aging at 1073 K showed no phase transformation.
- The crystallite size generally decreased with performing the aging process for 1 h.

**Acknowledgements** This work has been supported by the Management Unit of Scientific Research Projects of Firat University (FUBAP) (Project Number: FF.19.06).

## References


Acar E, Kok M, Qader I (2020) Exploring surface oxidation behavior of NiTi–V alloys. Eur Phys J Plus 135:58. https://doi.org/10.1140/epjp/s13360-019-00087-y

Araujo APMD, Simões JDB, Araújo CJD (2017) Analysis of compositional modification of commercial aluminum bronzes to obtain functional shape memory properties. Mater Res 20:331–341. https://doi.org/10.1590/1980-5373-mr-2016-1012

Balo ŞN, Sel N (2012) Effects of thermal aging on transformation temperatures and some physical parameters of Cu–13.5 wt.% Al–4 wt.% Ni shape memory alloy. Thermochim Acta 536:1–5. https://doi.org/10.1016/j.tca.2012.02.007

Benke M, Mertinger V, Nagy E, Van Humbeeck J (2007) Investigation of ageing phenomena in CuAlNi based shape memory alloys. In: Paper presented at the materials science forum

Braga FDO, Matlakhov AN, Matlakhova LA, Monteiro SN, Araújo CJD (2017) Martensitic transformation under compression of a plasma processed polycrystalline shape memory CuAlNi alloy. Mater Res 20:1579–1592. https://doi.org/10.1590/1980-5373-mr-2016-0476

Buytoz S, Dagdelen F, Qader I, Kok M, Tanyildizi B (2019) Microstructure analysis and thermal characteristics of NiTiHf shape memory alloy with different composition. Met Mater Int. https://doi.org/10.1007/s12540-019-00444-7

Čolić M, Rudolf R, Stamenković D, Anžel I, Vučević D, Jenko M, Lojen G (2010) Relationship between microstructure, cytotoxicity and corrosion properties of a Cu–Al–Ni shape memory alloy. Acta Biomater 6:308–317. https://doi.org/10.1016/j.actbio.2009.06.027

Dagdelen F, Aldalawi MAK, Kok M, Qader IN (2019a) Influence of Ni addition and heat treatment on phase transformation temperatures and microstructures of a ternary CuAlCr alloy. Eur Phys J Plus 134:66. https://doi.org/10.1140/epjp/i2019-12479-3

Dagdelen F, Kok M, Qader I (2019b) Effects of Ta content on thermodynamic properties and transformation temperatures of shape memory NiTi alloy. Met Mater Int. https://doi.org/10.1007/s12540-019-00298-z

Dagdelen F, Esra B, Qader IN, Ozen E, Kok M, Kanca MS, Mohammed SS (2020) Influence of the Nb content on the microstructure and phase transformation properties of NiTiNb shape memory alloys. JOM 72:1664–1672. https://doi.org/10.1007/s11837-020-04026-6

Elrasasi T, Dobróka M, Daróczi L, Beke D (2013) Effect of thermal and mechanical cycling on the elastic and dissipative energy in CuAl (11.5 wt%) Ni (5.0 wt%) shape memory alloy. J Alloys Compd 577:S517–S520. https://doi.org/10.1016/j.jallcom.2012.06.108

Ercan E, Dagdelen F, Qader I (2020) Effect of tantalum contents on transformation temperatures, thermal behaviors and microstructure of CuAlTa HTSMAs. J Therm Anal Calorim 139:29–36. https://doi.org/10.1007/s10973-019-08418-y

Graesser E, Cozzarelli F (1991) Shape-memory alloys as new materials for aseismic isolation. J Eng Mech 117:2590–2608. https://doi.org/10.1061/(ASCE)0733-9399(1991)117:11(2590)

Ii S, Tsuchiya K, Koyano T (2009) Aging effect on martensitic transformation at cryogenic temperatures in Cu–Al–Mn alloy. In: Paper presented at the European symposium on martensitic transformations

Kok M, Al-Jaf AOA, Çirak ZD, Qader IN, Özen E (2019) Effects of heat treatment temperatures on phase transformation, thermodynamical parameters, crystal microstructure, and electrical resistivity of NiTiV shape memory alloy. J Therm Anal Calorim. https://doi.org/10.1007/s10973-019-08788-3

Kök M, Qader IN, Mohammed SS, Öner E, Dağdelen F, Aydogdu Y (2020) Thermal stability and some thermodynamics analysis of heat treated quaternary CuAlNiTa shape memory alloy. Mater Res Express. https://doi.org/10.1088/2053-1591/ab5bef

Mabe J (2008) Variable area jet nozzle for noise reduction using shape memory alloy actuators. J Acoust Soc Am 123:3871

Moghaddam AO, Mazinani A, Ketabchi M (2017) Effect of accumulative roll bonding and equal channel angular rolling on microstructural and mechanical properties of Cu–Al–Mn shape memory alloys. Trans Indian Inst Met 70:1901–1909. https://doi.org/10.1007/s12666-016-1007-4

Otsuka K, Sakamoto H, Shimizu K (1979) Successive stress-induced martensitic transformations and associated transformation pseudoelasticity in Cu–Al–Ni alloys. Acta Metall 27:585–601. https://doi.org/10.1016/0001-6160(79)90011-7

Qader IN, Kök M, Dağdelen F (2019a) Effect of heat treatment on thermodynamics parameters, crystal and microstructure of (Cu–Al–Ni–Hf) shape memory alloy. Phys B 553:1–5. https://doi.org/10.1016/j.physb.2018.10.021

Qader IN, Kök M, Dağdelen F, Aydogdu Y (2019b) A review of smart materials: researches and applications. El-Cezerî J Sci Eng 6:755–788. https://doi.org/10.31202/ecjse.562177

Recarte V, Pérez-Landazábal J, Rodrıguez P, Bocanegra E, Nó M, San Juan J (2004) Thermodynamics of thermally induced martensitic transformations in Cu–Al–Ni shape memory alloys. Acta Mater 52:3941–3948. https://doi.org/10.1016/j.actamat.2004.05.009

Saud SN, Hamzah E, Abubakar T, Bakhsheshi-Rad H, Hosseinian R (2016) X-phase precipitation in aging of Cu–Al–Ni–xTi shape memory alloys and its influence on phase transition behavior. J Therm Anal Calorim 123:377–389. https://doi.org/10.1007/s10973-015-4894-4

Shiva S, Palani I, Mishra S, Paul C, Kukreja L (2015) Investigations on the influence of composition in the development of Ni–Ti shape memory alloy using laser based additive manufacturing. Opt Laser Technol 69:44–51. https://doi.org/10.1016/j.optlastec.2014.12.014

Suresh N, Ramamurty U (2008) Aging response and its effect on the functional properties of Cu–Al–Ni shape memory alloys. J Alloy Compd 449:113–118. https://doi.org/10.1016/j.jallcom.2006.02.094

Tatar C, Acar R, Qader IN (2020) Investigation of thermodynamic and microstructural characteristics of NiTiCu shape memory alloys produced by arc-melting method. Eur Phys J Plus 135:311. https://doi.org/10.1140/epjp/s13360-020-00288-w

Vajpai S, Dube R, Sangal S (2013) Application of rapid solidification powder metallurgy processing to prepare Cu–Al–Ni high temperature shape memory alloy strips with high strength and high ductility. Mater Sci Eng A 570:32–42. https://doi.org/10.1016/j.msea.2013.01.063

Zhou Z, Cui J, Ren X (2017) Phase diagram of FeNiCoAlTaB ferrous shape memory alloy on aging time. AIP Adv 7:045019. https://doi.org/10.1063/1.4982695